

EVOLUTION OF ANISOTROPY OF SHEET METALS DURING PLASTIC DEFORMATION

M. Safaei¹, W. De Waele¹

¹ Ghent University, Laboratory Soete, Belgium

Abstract: Sheet metals generally exhibit a considerable anisotropy due to their crystallographic texture. The mechanical anisotropic characteristics of the sheet metal have a great influence on the shape of the specimen after the deformation. Therefore many successful phenomenological models have been proposed for use in Finite Element (FE) codes to simulate the anisotropic behavior of a material. The anisotropy is mainly described on the basis of the initial Lankford coefficients and/or yield stresses along the orthotropic (rolling and transverse) and diagonal axes of the sheet metals. The different yield functions make use of different combinations of these constant parameters to represent a 3-dimensional surface (in case of plane stress) determining the transition between elastic and plastic deformation. Generally, the evolution of anisotropy is not considered in the formulation of a constitutive model. Therefore we studied the effects of plastic work on the evolution of anisotropic behavior. The experiments consist of conventional tensile testing of specimens taken at different orientations with respect to the rolling direction. Strain measurements are performed by means of an optical measurement technique. A simple (but powerful) technique for considering distortional anisotropy applicable to any yield criterion is presented. This technique is based on the polynomial definition for instantaneous Lankford coefficient combined with Newton-Raphson iteration. The same approach is applied for evolution of yield stress.

Keywords: Metal characterization; Digital image correlation; Lankford coefficient; Anisotropy; Deep drawing steels

1 INTRODUCTION

In this study we used, besides a conventional mechanical extensometer, the Digital Image Correlation (DIC) technique to measure strains in longitudinal and transverse directions. This technique is suitable for full-field, non-contact measurement of 3D deformations. A stochastic pattern of black and white speckles is produced at the specimens' surface by spray painting. Software based on a dedicated image correlation algorithm is used to process the images recorded by two synchronized digital cameras. A considerable advantage of using DIC as compared to a mechanical extensometer for strain measurement is that data can be extracted beyond the onset of necking.

We aim to propose a simple approach to describe the evolution of Lankford coefficients and yield stresses at different orientations as a function of plastic work. The outcome of the proposed formulation will be the prediction of yield/plastic potential locus with respect to plastic deformation. Furthermore, the anisotropic parameters of the yield function can be updated at any step of a finite element simulation. The iteration scheme required for the proposed approach is also described.

2 INITIAL MATERIALS CHARACTERIZATION

The true stress versus longitudinal plastic strain curves are shown in Figure 1. Those data were used to determine the Voce isotropic hardening coefficients. The Voce isotropic hardening law for any orientation θ with respect to RD is written as

$$\sigma_{\theta}^y = \sigma_{\theta}^0 + Q_{\theta}(1 - \text{EXP}(-b_{\theta}\bar{\epsilon}^p)) \quad (1)$$

where σ_{θ}^y and $\bar{\epsilon}^p$ respectively denote flow stress and effective plastic strain and σ_{θ}^0 , Q_{θ} and b_{θ} being hardening parameters depending on the material. The calculated parameters are summarized in Table 1 for seven orientations.

The plastic strain ratio, Lankford coefficient, is defined by the ratio of width to thickness plastic strain increments. However, due to practical difficulties associated with the direct measurement of thickness strains in sheet metals, this quantity is calculated based on the incompressibility hypothesis and using increments of plastic strains at tensile loading direction θ and at direction $90^{\circ} + \theta$, denoted respectively by $d\epsilon_{\theta}^p$ and $d\epsilon_{90^{\circ}+\theta}^p$. Therefore the definition of Lankford coefficient writes

$$R_{\theta} = -d\epsilon_{90+\theta}^p / (d\epsilon_{90+\theta}^p + d\epsilon_{\theta}^p) \tag{2}$$

In accordance with ISO 10113 the linear regression of width versus length true plastic strain plot between a lower and upper limit of plastic strain is used to calculate the Lankford coefficient. In this study we chose 0 and 0.2 respectively for lower and upper limit of plastic strain. The experimental width versus length plastic strains are plotted in Figure 2 for seven orientations θ . If the gradient to (the linear curve fits of) these curves is m , then the Lankford coefficient R at orientation θ is obtained by

$$R_{\theta} = -m_{\theta} / (1 + m_{\theta}) \tag{3}$$

Table 2 shows the Lankford coefficients obtained by equation(3). The variation of Lankford coefficient for different directions is depicted in Figure 3.

Normal and planar anisotropy coefficients are defined respectively in equations (4) and (5)

$$R_n = (R_0 + 2R_{45} + R_{90}) / 4 \tag{4}$$

$$\Delta R = (R_0 - 2R_{45} + R_{90}) / 2 \tag{5}$$

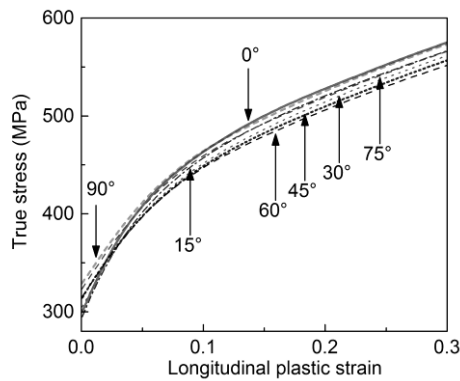


Figure 1. Stress-strain data at 7 orientations with respect to rolling direction.

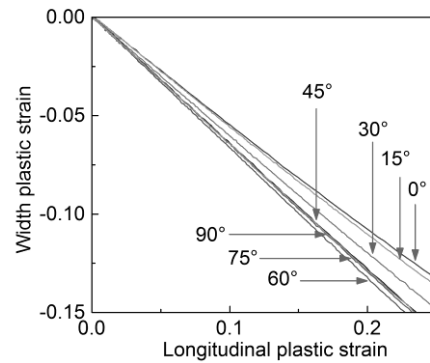


Figure 2. Experimental width to length plastic strains.

Normal anisotropy relates to the average width to thickness reduction; thus higher r_n means less thinning and better formability. On the other hand, higher planar anisotropy means more anisotropic behaviour. This anisotropic behavior can simply be observed as earing profile in a deep drawn cylindrical cup. The measured values of normal and planar anisotropy are given in Table 2.

Table 1. Voce isotropic hardening coefficients

	0°	15°	30°	45°	60°	75°	90°
Q [MPa]	251.46	248.86	245.34	236.66	228.40	236.85	239.0
b [-]	10.84	10.70	9.24	8.54	8.841	8.68	8.54
σ_0 [MPa]	299.54	295.93	304.81	313.47	313.52	321.83	326.64

Table 2. Linear Lankford coefficient at different orientations, planar and normal anisotropy coefficient

Orientation (θ)	0°	15°	30°	45°	60°	75°	90°	ΔR	R_n
R_{θ}	1.21	1.27	1.52	1.81	1.99	1.86	1.83	-0.29	1.66

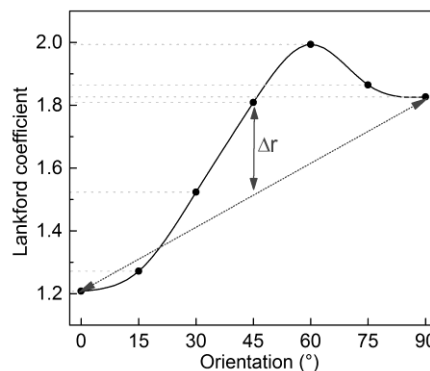


Figure 3. Experimentally determined Lankford coefficients obtained from equation (3).

3 HILL'S QUADRATIC YIELD FUNCTION AS AN EXAMPLE

Starting from Hill's 48 quadratic anisotropy model, various yield functions have been proposed to describe the initial anisotropy of metallic sheets mainly based on the assumption of an associated flow rule. The material coefficients of the anisotropic yield functions commonly need to be calibrated from experimental tensile, shear or bi-axial yield stresses and Lankford coefficients in order to accurately describe both yielding and plastic flow behavior of metallic sheets. As an example, the Hill's 48 quadratic yield function was chosen for further study. The yield criteria is described by

$$f - \sigma_0^y = 0 \quad (6)$$

f and σ_0^y respectively being yield and reference isotropic hardening functions. The rolling direction is mainly used as reference direction in the above equation. Two forms of yield function f have been widely implemented in finite element software. They are distinguished by the way that their parameters are calibrated. One way of parameter calibration is solely based on Lankford coefficients at 0° , 45° and 90° (R_0 , R_{45} and R_{90}). This case is referred to as R-based Hill's 48. Alternatively the yield function can be identified by directional yield stresses, it is then called S-based model. The R-based and S-based Hill's 48 are written respectively as

$$f_p = (\sigma_{11}^2 + \lambda_p \sigma_{22}^2 - 2\nu_p \sigma_{11} \sigma_{22} + 2\rho_p \sigma_{12}^2)^{1/2} \quad (7)$$

$$f_y = (\sigma_{11}^2 + \lambda_y \sigma_{22}^2 - 2\nu_y \sigma_{11} \sigma_{22} + 2\rho_y \sigma_{12}^2)^{1/2} \quad (8)$$

The subscripts p and y are respectively chosen for R-based and S-based model to avoid confusion. The coefficients of the above equations are defined as

$$\lambda_p = \frac{R_0(1+R_{90})}{R_{90}(1+R_0)} \quad ; \quad \nu_p = \frac{R_0}{1+R_0} \quad ; \quad \rho_p = \frac{(R_0+R_{90})(1+2R_{45})}{2R_{90}(1+R_0)} \quad (9)$$

$$\lambda_y = \left(\frac{\sigma_0}{\sigma_{90}}\right)^2 \quad ; \quad \nu_y = \frac{1}{2} \left(1 + \left(\frac{\sigma_0}{\sigma_{90}}\right)^2 - \left(\frac{\sigma_0}{\sigma_b}\right)^2\right) \quad ; \quad \rho_y = 2 \left(\frac{\sigma_0}{\sigma_{45}}\right)^2 - \frac{1}{2} \left(\frac{\sigma_0}{\sigma_b}\right)^2$$

σ_0 , σ_{45} , σ_{90} and σ_b being initial yield stresses at 0° , 45° , 90° and equi-biaxial state.

Assuming the associated flow rule, the gradient of the yield surface describes the direction of plastic flow, D^p (Figure 4). This hypothesis is referred to as normality rule; for associated plasticity models we write

$$d\varepsilon^p = d\bar{\varepsilon}^p D^p \quad (10)$$

where $d\varepsilon^p$ and $\bar{d\varepsilon}^p$ respectively denote plastic strain rate and effective plastic strain. D^p is the first gradient of the yield locus determining the outward normal vector to the same locus.

In order to study the shape of the yield locus and furthermore the direction of plastic strain rate, we agree on using plastic work contours. As a general practice, we use rolling direction as reference direction. The true stress and corresponding plastic work per unit volume (W_p or specific plastic work) is determined at a specific true plastic strain. Subsequently, the true stress values (σ_θ) corresponding to the same value of specific plastic work were determined for different orientations. Those stresses at the same level of specific plastic work, when plotted in stress space, represent the specific plastic work contour. The initial normalized yield surface for IF300 is plotted in Figure 4.

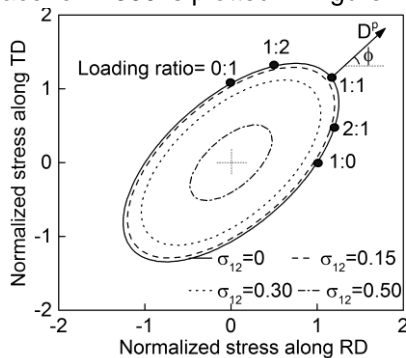


Figure 4. Initial yield surface depicting the specific plastic work contour $W_p = 0$ using Hill's 48 R-based.

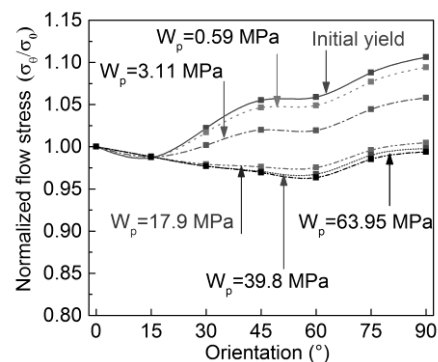


Figure 5. Normalized flow stresses for seven orientations at different levels of specific plastic work.

The shape of the yield surface and consequently the plastic strain rate direction (D^p) will remain unchanged during the plastic deformation if the anisotropic hardening parameters are kept fixed at their initial values. Using the normality rule described in equation (10) we can find the φ angle which the plastic strain rate vector makes with the rolling axis for different biaxial loading ratios. Therefore:

$$\begin{aligned}\tan(\varphi_{1:0}) &= -\frac{R_0}{1+R_0} \\ \tan(\varphi_{2:1}) &= \frac{R_0(1-R_{90})}{R_{90}(2+R_0)} \\ \tan(\varphi_{1:1}) &= \frac{R_0}{R_{90}} \\ \tan(\varphi_{1:2}) &= \frac{R_0(2+R_{90})}{R_{90}(1-R_0)} \\ \tan(\varphi_{0:1}) &= -\frac{1+R_{90}}{R_0}\end{aligned}\quad (11)$$

4 ANISOTROPY EVOLUTION IN TERMS OF YIELD STRESS

4.1 Experimental observations

Generally when isotropic hardening is used, it is assumed that the relation between yield stresses at different orientation and that of the reference orientation (0°) remains constant, thus proportional expansion of the yield surface happens by increase of plastic strain. Thus, the shape of the yield surface is constant regardless of the level of plastic work. The normalized yield stresses, σ_θ/σ_0 , determined by specific plastic work equivalence, must coincide for different levels of specific plastic work.

However, it can be observed in Figure 1 that the initial proportionality of the hardening rate changes upon further plastic deformation. The normalized yield stress values at different specific plastic work levels are plotted in Figure 5. Due to the observed change of normalized yield stresses with plastic deformation, a variation of anisotropy coefficients can be expected. The evolution of anisotropy coefficients of the S-based Hill's 48 model described in equations (8) and (9) is plotted in Figure 6 and presented in Table 3 for different levels of plastic work.

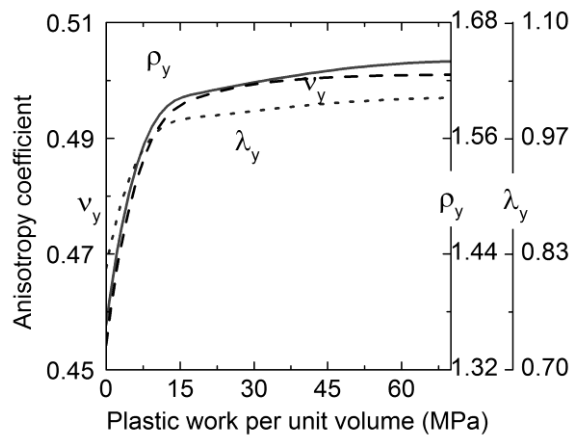


Figure 6. Evolution of anisotropy coefficients of Hill's 48 S-based model with respect to specific plastic work.

Table 3. Anisotropy parameters with respect to plastic work per unit volume

Plastic strain	Wp	v_p	ρ_p	λ_p	v_y	ρ_y	λ_y
0.00	0.00	0.56	1.70	0.87	0.46	1.35	0.82
0.00	0.60	0.56	1.71	0.87	0.46	1.37	0.84
0.01	3.11	0.56	1.71	0.86	0.47	1.45	0.89
0.05	17.93	0.55	1.73	0.85	0.50	1.60	0.99
0.10	39.83	0.54	1.74	0.84	0.50	1.62	1.00
0.15	63.95	0.53	1.74	0.83	0.50	1.63	1.01
0.20	89.65	0.52	1.73	0.82	0.50	1.62	1.01
0.25	116.67	0.50	1.72	0.81	0.50	1.61	1.01
0.30	144.85	0.48	1.69	0.81	0.50	1.60	1.01

A pronounced change in the anisotropy coefficients is observed up to a specific plastic work value of 15MPa. However, this variation becomes less pronounced at higher specific plastic work values. For this reason Yoon and Barlat proposed using yield stress values at high plastic work [1].

4.2 Review of some methods

In the previous section, it is experimentally demonstrated that hardening rates at different orientations change with respect to specific plastic work for the studied steel IF300. A similar conclusion was reported for steel types DC06 and HSLA320 in the work of Safaei et al [2]. Also, Yoon et al [3] showed that for AA5042-H2 aluminum alloys there is a considerable change in the hardening rates measured in equi-biaxial and uniaxial stress tests.

Different attempts were taken to model this distortional hardening behavior. For instance, Stoughton and Yoon [4] proposed a non-associated flow model in which the hardening at 0°, 45°, 90° uniaxial stress and equi-biaxial stress state are explicitly incorporated into the Hill's 48 yield stress function. A significant improvement was reported, especially for the prediction of biaxial hardening for stainless steels 719-B and 718-AT, and aluminum alloys AA 5182-O and AA 6022-T4E32 even when compared with the non-quadratic Yld2000-2d anisotropic yield function. Aretz [5] proposed a yield function based on linear transformation of stress tensors in which the yield stress at different orientations is determined by an equivalent plastic work theorem incorporated in his material model. Abedrabbo [6, 7] used third and fifth order polynomial functions to predict the variation of anisotropy coefficient with respect to temperature. Wang updated the Yld2000-2d parameters with effective plastic strain using sixth order polynomial functions [8]. Hu introduced a formulation in his yield criterion in which directional hardenings were described explicitly [9].

If $\bar{\varepsilon}_n^p$ is the effective plastic strain at the last converged step, then the plastic work per unit volume corresponding to that value is

$$W_p^* = \int_0^{\bar{\varepsilon}_n^p} \sigma_0^y d\bar{\varepsilon}^p \quad (12)$$

In the next step, directional effective plastic strains $\bar{\varepsilon}_\theta^p$ at required directions (θ) along the rolling axis (0°) corresponding to the known magnitude of plastic work W_p^* are iteratively calculated.

We define a residual function such as g_θ where

$$g_\theta = W_p^\theta - W_p^* \quad (13)$$

W_p^θ being the plastic work at $\bar{\varepsilon}_\theta^p$ that iteratively reaches to W_p^* using the Newton-Raphson iteration method. On other words, the $\bar{\varepsilon}_\theta^p$ is determined in a way that the difference between $\bar{\varepsilon}_\theta^p$ in ($k + 1$)-th and k -th iterations is less than a defined tolerance.

$$\bar{\varepsilon}_\theta^{p(k+1)} = \bar{\varepsilon}_\theta^{p(k)} - g_\theta / g'_\theta \quad (14)$$

and

$$g'_\theta = \partial g_\theta / \partial \bar{\varepsilon}_\theta^p = \sigma_\theta^y \quad (15)$$

Next, the directional plastic strains $\bar{\varepsilon}_\theta^p$ corresponding to the same level of specific plastic work W_p^* are calculated and those values are used in the isotropic hardening law in equation (1) using corresponding parameters in Table I. We use these $\bar{\varepsilon}_\theta^p$ to obtain the instantaneous Lankford coefficients.

5 ANISOTROPY EVOLUTION IN TERMS OF PLASTIC STRAIN RATIOS

Compared to the number of research papers studying hardening induced anisotropy, less research has been done in order to describe the evolution of the yield surface by incorporating Lankford coefficients changing with specific plastic work. Hu used a series of explicit formulations for directional Lankford coefficients in his anisotropic yield criterion [9]. In this paper we propose a simple method that can be implemented into finite element codes conveniently.

We described that commonly a constant Lankford coefficient is used in the phenomenological anisotropic models. Nonetheless this common assumption, variations in the Lankford coefficients were observed in our experimental data, Figure 7.

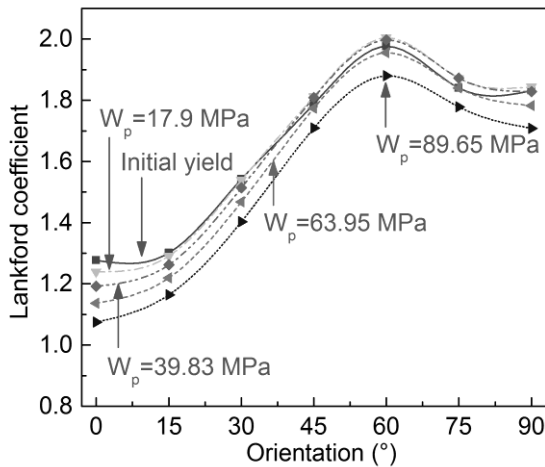


Figure 7. Lankford coefficient at different level of plastic work.

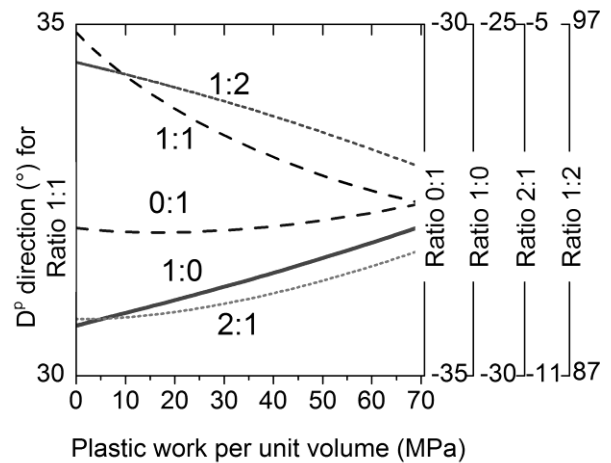


Figure 8. Evolution of direction of plastic strain rate against rolling axis as a function of specific plastic work.

We mentioned earlier that in the framework of an associated flow rule the normality hypothesis determines the direction of plastic strain rate. In other words, the outward normal to the yield locus makes an angle with the rolling direction that can be calculated using the gradient of yield locus. This angle remains unchanged when the loading direction is constant and is given in equation (11) for various loading ratios when Hill's 48 R-based function is considered. However, some changes in the angle of plastic strain rate vector against rolling axis is detected in the experimental results, see Figure 8. These angles are calculated substituting instantaneous Lankford coefficients at 0°, 45° and 90° into equation (11). These values are also substituted in equation (9), to determine the evolution of anisotropy parameters, Figure 9 and Table 3.

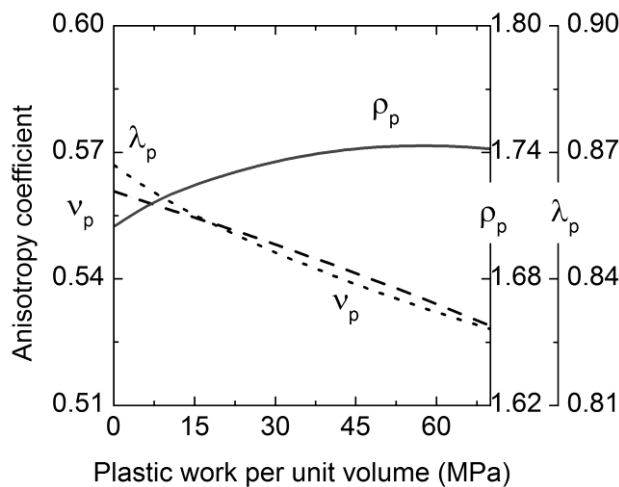


Figure 9. Evolution of anisotropy coefficients of Hill's 48 R-based function as a function of specific plastic work.

As described earlier, a constant value for Lankford coefficient can be obtained by linear curve fitting of the width to length strain data. However, the experimental curves plotted in Figure 3 can be more accurately described by a higher order polynomial, e.g., 3rd order. Therefore we use the derivative (m_θ) of that polynomial function in the following equation

$$R_\theta(\bar{\epsilon}_\theta^p) = -\frac{m_\theta(\bar{\epsilon}_\theta^p)}{1+m_\theta(\bar{\epsilon}_\theta^p)} \quad (16)$$

with $m_\theta(\bar{\epsilon}_\theta^p)$ is a 2nd order polynomial function. Note that the calculation of $\bar{\epsilon}_\theta^p$ was defined in the previous section using Newton-Raphson iteration. We write $m_\theta(\bar{\epsilon}_\theta^p)$ in general form as

$$m_\theta(\bar{\epsilon}_\theta^p) = \alpha_\theta^{(1)} + 2\alpha_\theta^{(2)}\bar{\epsilon}_\theta^p + 3\alpha_\theta^{(3)}(\bar{\epsilon}_\theta^p)^2 \quad (17)$$

where $\alpha_\theta^{(1)}$, $\alpha_\theta^{(2)}$ and $\alpha_\theta^{(3)}$ are polynomial parameters corresponding to angle θ . These parameters are presented in Table IV.

Summarizing, at any given effective plastic strain of $\bar{\varepsilon}^p$ corresponding to W_p^* in equation (12) the directional effective plastic strain $\bar{\varepsilon}_\theta^p$ in θ direction is iteratively determined using the approach described in equations (13)-(15). Next, the instantaneous gradient of width to length plastic strain denoted by $m_\theta(\bar{\varepsilon}_\theta^p)$ is determined using equation (17) and parameters available in Table 4. Consequently the instantaneous Lankford coefficient is updated using $R_\theta(\bar{\varepsilon}_\theta^p)$ in equation (16) and previously determined $m_\theta(\bar{\varepsilon}_\theta^p)$. Finally the Hill'48 R-based yield locus (equation (7)) is calculated using the $R_\theta(\bar{\varepsilon}_\theta^p)$ and parameters in equation (9).

Using this approach, yield stress contours at different specific plastic work levels are plotted in Figure 10. Note that the stresses in Figure 10 are normalized by the reference yield stress (in the rolling direction). It is interesting to note that the subsequent yield loci present a noticeable change in shape.

Table 4. Parameters of 2nd order polynomial defined in equation (17)

Orientation (θ)	0°	15°	30°	45°	60°	75°	90°
$\alpha^{(1)}$	-0.561	-0.566	-0.607	-0.641	-0.664	-0.648	-0.647
$\alpha^{(2)}$	0.064	0.006	-0.011	-0.052	-0.050	-0.058	-0.036
$\alpha^{(3)}$	0.144	0.207	0.219	0.252	0.252	0.258	0.254

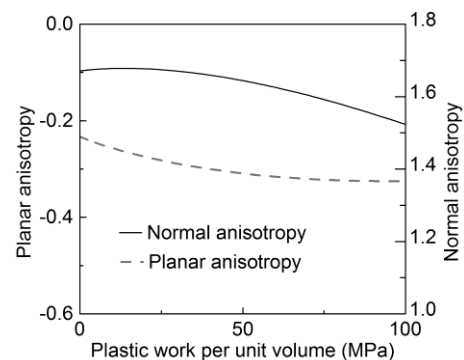
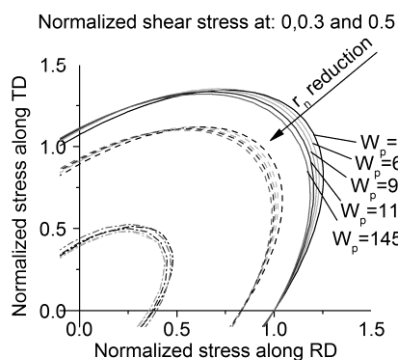


Figure 10. Contours of plastic work based on Hill's 48 R-based model.

Figure 11. Evolution of planar and normal anisotropy quantities as a function of plastic work.

Evolution of normal and planar anisotropy with regard to plastic work per unit volume is plotted in Figure 11. It can be concluded that using the anisotropy coefficients at higher levels of specific plastic work instead of initial values, both earing generation and formability of the material decreases. The reduction in the formability of the material (reduction in normal anisotropy) observed in Figure 11 can be correlated to the contracted shape of the yield locus at 1:1 loading ratio.

6 SUMMARY

In this paper, the evolution of anisotropy behavior of the interstitial free steel IF300 with respect to specific plastic work was studied. To this end, tensile tests at seven different directions were carried out. Longitudinal and width strains were measured by means of digital image correlation. It was shown that proportionality of yield stress values at large strains does not conform that of the initial yield state. Thus a method was reviewed that calculates the instantaneous yield stresses according to the real isotropic hardening for directions used in the yield model. The described method makes use of the Newton-Raphson iteration scheme to find the directional effective plastic strains corresponding to a similar level specific plastic work. This method has already been used in previous studies.^{17,19} We employed a similar approach to calculate instantaneous Lankford coefficients at any value of specific plastic work. First, we described directional Lankford coefficient as a polynomial function. Next, we used the calculated directional effective plastic strains in that function. Based hereon we showed the both yield stress and plastic potential functions can be updated with respect to specific plastic work..

7 ACKNOWLEDGEMENTS

Acknowledgement. The financial support from the Ghent University Research Fund (BOF08/24J/106) is greatly appreciated.

8 REFERENCES

- [1] Yoon JW, Barlat F. Modeling and simulation of the forming of aluminum sheet alloys. In: Semiatin SL, editor. ASM handbook, vol. 14B. ASM International, 2006. p.792.
- [2] Safaei M, De Waele W, Hertschap K. Characterization of Deep Drawing Steels Using Optical Strain Measurements. Steel Research International 2012;in press.
- [3] Yoon J-H, Cazacu O, Whan Yoon J, Dick RE. Earing predictions for strongly textured aluminum sheets. International Journal of Mechanical Sciences 2010;52:1563.
- [4] Stoughton TB, Yoon JW. Anisotropic hardening and non-associated flow in proportional loading of sheet metals. International Journal of Plasticity 2009;25:1777.
- [5] Aretz H. A simple isotropic-distortional hardening model and its application in elastic-plastic analysis of localized necking in orthotropic sheet metals. International Journal of Plasticity 2008;24:1457.
- [6] Abedrabbo N, Pourboghrat F, Carsley J. Forming of aluminum alloys at elevated temperatures - Part 1: Material characterization. International Journal of Plasticity 2006;22:314.
- [7] Abedrabbo N, Pourboghrat F, Carsley J. Forming of aluminum alloys at elevated temperatures - Part 2: Numerical modeling and experimental verification. International Journal of Plasticity 2006;22:342.
- [8] Wang H, Wan M, Wu X, Yan Y. The equivalent plastic strain-dependent Yld2000-2d yield function and the experimental verification. Computational Materials Science 2009;47:12.
- [9] Hu W. Constitutive modeling of orthotropic sheet metals by presenting hardening-induced anisotropy. International Journal of Plasticity 2007;23:620.